Available online at www.sciencedirect.com
ScienceDirect
Trans. Nonferrous Met. Soc. China 25(2015) 1917−1925
Transactions of Nonferrous Metals Society of China
www.tnmsc.cn

Corrosion resistance of in-situ Mg−Al hydrotalcite conversion film on AZ31 magnesium alloy by one-step formation

Rong-chang ZENG[1,2], Zhen-guo LIU[1,2], Fen ZHANG[1,2], Shuo-qi LI[1,2], Qing-kun HE[1], Hong-zhi CUI[1], En-hou HAN[3]

1. College of Materials Science and Engineering, Shandong University of Science and Technology, Qingdao 266590, China;
2. State Key Laboratory of Mining Disaster Prevention and Control Co-founded by Shandong Province and the Ministry of Science and Technology, Shandong University of Science and Technology, Qingdao 266590, China;
3. Institute of Metals Research, Chinese Academy of Sciences, Shenyang 110016, China

Received 25 July 2014; accepted 10 December 2014

Abstract: In situ growth of nano-sized layered double hydroxides (LDH) conversion film on AZ31 alloy was synthesized by a urea hydrolysis method. The formation mechanism of the film was proposed. Firstly, the dissolved Mg^{2+} ions deposited into a precursor film consisted of $MgCO_3$ and $Mg_5(CO_3)_4(OH)_2\cdot 4H_2O$; secondly, the precursor translated into the crystalline $Mg(OH)_2$ in alkaline conditions; finally, the Mg^{2+} ions in $Mg(OH)_2$ were replaced by Al^{3+} ions, $Mg(OH)_2$ translated into the more stable LDH structure, simultaneously, the OH^- ions in the interlayer were exchanged by CO_3^{2-}, thus led to the formation of the LDH ($Mg_6Al_2(OH)_{16}CO_3\cdot 4H_2O$) film. The results indicated that the LDH film characterized by interlocking plate-like nanostructures and ion-exchange ability significantly improved the corrosion resistance of the AZ31 Mg alloy.

Key words: magnesium alloy; hydrotalcite; conversion film; corrosion resistance; ion-exchange

1 Introduction

Magnesium and its alloys exhibit excellent physical and mechanical properties such as high specific strength, low density and good electromagnetic shielding characteristics, rendering them appropriate for application in automobile, aerospace, communications and computer industry [1−3]. Their poor corrosion resistance, however, has limited their use. Therefore, it is of great importance to improve the corrosion resistance of magnesium alloys [4]. Protective films are normally applied on magnesium surfaces to provide a dense barrier against the corrosive species [5]. Various surface treatments including chemical conversion [6], microarc oxidation (MAO) [7,8], electrodeposition [9] and polymeric coating [10] have been developed on magnesium alloys to improve their corrosion resistance. Among these surface treatments, chemical conversion coatings are regarded as effective measures to enhance the corrosion resistance of magnesium alloys. Unfortunately, some conversion coatings, for instance, chromate coatings [11], phosphate coatings [12] and vanadia coatings [13], can cause environmental pollution and are harmful to people's health during manufacture and use. Thus, much work should be focused on developing an environmentally-friendly and corrosion-resistance conversion film on magnesium alloys.

Layered double hydroxides (LDHs), possess a special layered structure, which is similar to that of brucite, $Mg(OH)_2$. They are generally represented by the formula $[M^{2+}{}_{1-x},M^{3+}x(OH)_2]^{x+}(A)^{n-}{}_{x/2}\cdot mH_2O$, where M^{2+} and M^{3+} represent the divalent and trivalent cations, respectively, A^{n-} is the interlayer anion (such as CO_3^{2-}, NO_3^- or OH^-) and x has a value between 0.20 and 0.33 [14−17]. LDHs have been broadly applied because of their exchangeable anions and adjustable structures. The unique structure, the potent adsorption and ion-exchange capacity confer superior corrosion resistance to the LDHs films, which make LDHs become

Foundation item: Project (51241001) supported by the National Natural Science Foundation of China; Project (ZR2011EMM004) supported by Shandong Provincial Natural Science Foundation, China; Project (TS20110828) supported by Taishan Scholarship Project of Shandong Province, China; Project (2014TDJH104) supported by SDUST Research Fund, Joint Innovative Center for Safe and Effective Mining Technology and Equipment of Coal Resources of Shandong Province, China
Corresponding author: Rong-chang ZENG; Tel: +86-532-80681226; E-mail: rczeng@foxmail.com
DOI: 10.1016/S1003-6326(15)63799-2

the potential replacement for chromium conversion film [18−24]. Our research group [25,26] have prepared the nano-sized LDH ($Mg_6Al_2(OH)_{16}CO_3·4H_2O$) and LDHs ($Mg_6Al_2(OH)_{16}MoO_4·4H_2O$) coating with ion-exchange and self-healing ability by the co-precipitation and hydrothermal treatment on AZ31 Mg alloy. The corrosion resistance of the alloy was effectively improved. These coatings have the potential to act as smart coatings capable of response to the stimuli from environment. The in-situ growth process has been widely developed on pure aluminum, Al-based alloys and anodic aluminum oxide substrate to form Li−Al, Mg−Al, Ni−Al or Zn−Al LDH films [27,28]. Also, LIU et al [29] observed that LDH films can be fabricated on the Zn-covered stainless steel. The LDHs are usually formed in alkaline solution on the Al or Zn-based alloys because aluminum and zinc are active in the alkaline solutions whose pH values exceed 11, which can provide the source of M^{2+} or M^{3+} to form the LDH films. However, it is difficult to generate a LDH layer on the magnesium alloy surface, because magnesium is passive in alkaline solutions. A good process of the in-situ growth LDHs on magnesium in aqueous HCO_3^-/CO_3^{2-} medium was developed. The in-situ prepared Mg−Al and Mg−Fe hydrotalcite conversion films on AZ91 magnesium alloys and pure magnesium [18−20,23,24,30], exhibit high hydrophobicity and good corrosion resistance. Also, CHEN et al [14−17] adopted the in-situ method to prepare Mg−Al hydrotalcite on AZ31 alloy and then modified the hydrotalcite film with phytic acid. It is demonstrated that the LDH films lead to a significant enhancement in corrosion resistance of magnesium alloys. Nevertheless, there is still a drawback for the in-situ preparation of the Mg−Al−LDH films. The in-situ growth LDH conversion films are difficult and complex to be synthesized by one step in different solutions. Thus, the preparation of LDH films with high corrosion resistance and adhesion to the magnesium substrate by a simple technological process faces a challenge.

Urea solution with a neutral pH at room temperature can form a uniform solution with metal ions. However, when the temperature of the solution is higher than 90 °C, urea starts to hydrolyze and release large amounts of NH_3, thus increasing the solution pH value uniformly. Because of these advantages, urea is frequently used as homogeneous precipitating agent in the synthesis of LDHs [31,32]. Homogeneous precipitation of LDHs powder using urea hydrolysis is recognized as a method for obtaining well-crystallized, large LDHs powder [33,34]. Using the preparation of LDH powder for reference, the direct synthesis of LDH film on magnesium surface may be a feasible choice [35].

This work aims to prepare an in-situ growth LDH conversion film on the AZ31 Mg alloys using urea hydrolysis by a one-step method in autoclave. The characteristics of the LDH film and the corrosion resistance were investigated. The film formation mechanism was discussed, and a model for this mechanism was proposed.

2 Experimental

Commercial available cast AZ31 Mg alloys were used with nominal compositions of 3.0% Al, 1.0% Zn and balanced Mg. The ingot was cut into sizes of 20 mm × 20 mm × 4.0 mm. The samples were firstly ground to 2000 grit, and then ultrasonically cleaned in ethanol for 15 min, and finally dried by warm air. Urea and $Al(NO_3)_3·9H_2O$ with a mole ratio of urea to Al^{3+}=6:1, were dissolved in de-ionized water to give a mixture solution. Then, the above solution was transferred to a Teflon-lined autoclave in which the pretreated Mg alloy was immersed and then heated in a warm chamber at a temperature of 393 K for 5 h and 10 h. The resultant samples were rinsed with de-ionized water and dried at room temperature.

The structure and the composition of the films were characterized by an X-ray diffraction diffract meter (XRD, D/Max 2500PC) with Cu target (λ=0.154 nm) at a scanning rate of 0.02 (°)/s in the 2θ range of 5°−80°. The surface morphologies of the films were observed using a field-emission scanning electronic microscope (FE-SEM, Hitachi S−4800). The chemical compositions and cross section of the films were inspected through energy-dispersive X-ray spectrometer (EDS, Oxford Isis), which was affiliated by the electron probe X-ray microanalysis (EPMA, Oxford Isis). The obtained films were also probed using Fourier transform infrared spectroscopy (FT-IR, TENSOR−27) in the wavenumber range from 500 to 4000 cm^{-1} at room temperature. The corrosion resistance was evaluated by potentiodynamic polarization curves and electrochemical impedance spectrum (EIS) measurements. All electrochemical measurements were conducted in a classical three-electrode system which consists of the sample as the working electrode (1 cm^2), a platinum plate as the counter electrode and a saturated calomel electrode (SCE) as the reference electrode in 3.5% NaCl aqueous solution at room temperature using an electrochemical workstation (PARSTAT, 2273).

3 Results and discussion

The XRD patterns of the LDH films formed on AZ31 Mg alloy for different treatment time and the substrate are shown in Fig. 1. The XRD patterns of the samples treated by urea hydrolysis in autoclave treated

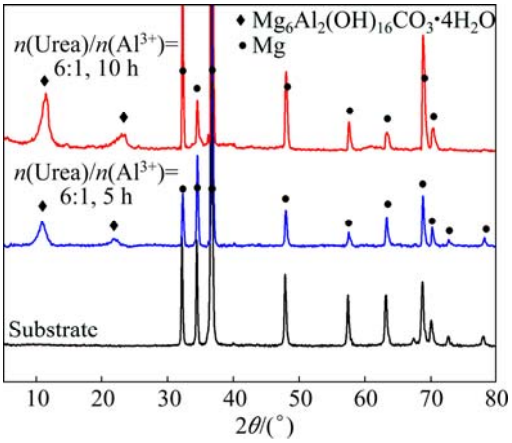

Fig. 1 XRD patterns of AZ31 substrate, LDH films treated for 5 h and 10 h

for 5 h and 10 h display the typical peaks of the LDH ($Mg_6Al_2(OH)_{16}CO_3·4H_2O$) phase at the 2$\theta$=10.9° and 22.1°, respectively. When the treatment time was prolonged, there was an obvious increase in the intensity of LDH phases. Meanwhile, some peaks attributed to the α-Mg phases decreased clearly in all the patterns. From the XRD results, it is concluded that the in-situ growth of Mg−Al hydrotalcite conversion film by urea hydrolysis in autoclave was successfully prepared on the AZ31 Mg alloy, and the crystallization intensity of the film was enhanced with the increasing treatment time.

The SEM images of the as-prepared LDH films (n(Urea)/n(Al^{3+})=6:1, 5 h) are shown in Fig. 2. Figure 2(a) demonstrates that the LDH film was compact over the whole AZ31 Mg alloy substrate. Figures 2(b)−(d) show that the LDH film possesses a typical LDH platelet-like microstructure. The detailed morphologies indicate that the LDH film has a compact, homogeneous and well-crystallized nanostructure with particle sizes of 100−150 nm. From Figs. 2(c) and (d), it can be seen that most of the LDH nano-sheets grew vertically cross-linked on the substrate and part of them were horizontally covered on the surface of the sample incompletely. The conversion film with compact and uniform structure, which can avoid the exposure of the substrate to the environment by effectively blocking the penetration of aggressive ions, has the potential to act as a corrosion-resistant film for Mg alloys.

The morphologies and their corresponding EDS spectra of the films (n(Urea)/n(Al^{3+})=6:1, 5 h) are shown in Fig. 3. The chemical compositions of the as-prepared film were analyzed by spot scanning. It can be seen in Fig. 3 that the as-prepared film is mainly composed of Mg, Al, O and C elements. The average mole ratio of Mg to Al is very close to 3: 1 (Table 1), indicating that the film mainly consisted of LDH ($Mg_6Al_2(OH)_{16}CO_3·4H_2O$). These EDS results agree well with the results of XRD patterns.

Further SEM observation on the cross section (n(Urea)/n(Al^{3+})=6:1, 5 h) (Fig. 4(a)) demonstrates the formation of a compact and thick LDH film. The film has two structural layers: a compact inner layer and a porous outer layer. The strong hydrogen evolution can also rupture the film and form some cracks. The exposed Mg substrate under the cracks can react with the

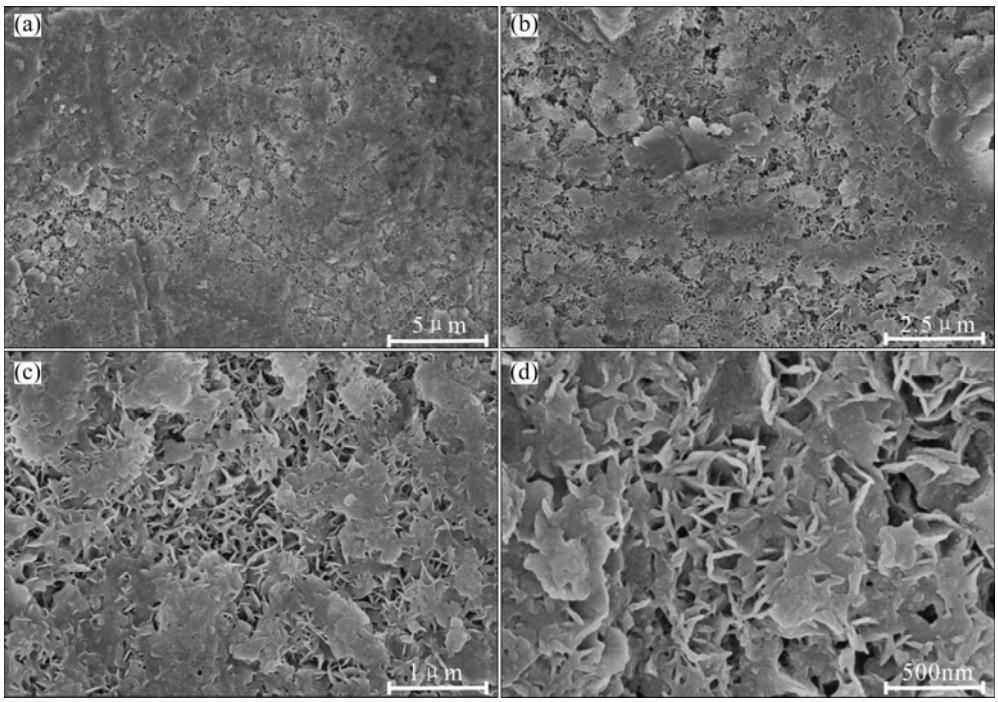

Fig. 2 SEM images of as-prepared LDH film (n(Urea)/n(Al^{3+})=6:1, 5 h) with different magnifications

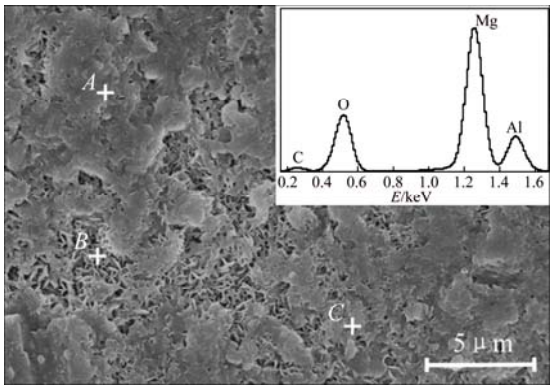

Fig. 3 Morphology and its corresponding EDS spectra of film

Table 1 Chemical composition of film probed by EDS

Element	Mole fraction/%			Average mole fraction/%
	A	*B*	*C*	
Mg	26.30	28.71	26.70	27.24
Al	8.60	8.63	10.44	9.22
O	51.02	48.36	52.09	50.49
C	14.07	14.30	10.76	13.04

pretreatment solution to form the porous outer layer of the film, which can make up the disadvantage of cracked film to a great extent. In addition, the dissolved Mg^{2+} ions from the substrate participate in the formation of the film. Therefore, the film can be formed in-situ on the surface of Mg alloy. By this method, strong adhesion can be achieved between the film and Mg substrate, which is sufficiently robust for the subsequent paint films or organic layers in the application. From the cross-sectional morphology (Fig. 4(a)), it can be seen that the LDH film is strongly adhered to Mg substrate. The film thickness of the compact layer is approximately 25−50 μm and that of the porous layer is 5−10 μm. The results demonstrate that the compact and uniform LDH film with strong adhesion can provide an effective protection to the Mg substrate.

The characteristic of the cross section was also analyzed with elemental mapping by EPMA (Fig. 4(b)). The elemental mapping results indicate that the film contained large amounts of Mg and O, and small amount of Al and C. The distributions of Mg, O and C ions in film were uniform, while the distribution of Al ions concentrated on the surface and the cracks of the film contacted with the solutions as well as the grain boundaries in the AZ31 substrate. Such aggregate phenomenon of Al element may be attributed to the Al^{3+} ions in the solution diffused into the cracks and the loose layer pores, which is difficult to clean thoroughly. These mapping results agree well with the results of spot scanning (Fig. 3) and XRD patterns (Fig. 1).

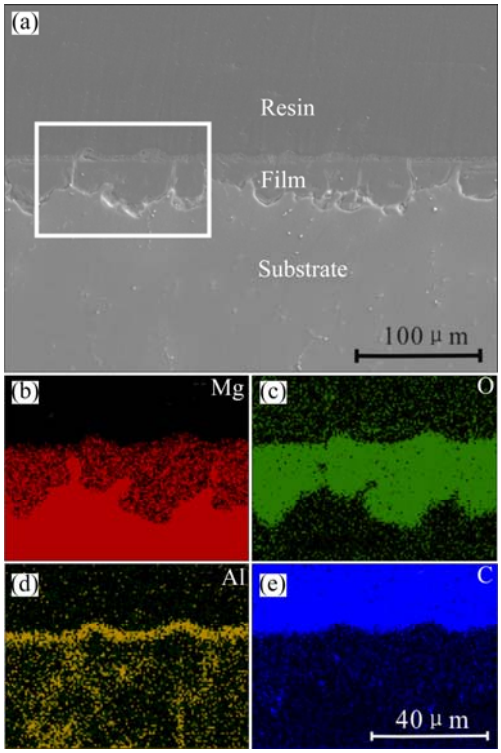

Fig. 4 Cross-section morphology (a) and elemental mapping (b, c, d, e) of LDH film

The FT-IR spectra of the as-prepared LDH films in different conditions are given in Fig. 5. The spectra show characteristic bands of the LDH [36,37]. The most predominant spectral feature is the intense sharp peak observed at 3460 cm^{-1}. The absorption band at 3460 cm^{-1} corresponds to O—H because of the presence of the surface absorption water, interlayer water and magnesia octahedron. The shoulder band at around 2921 cm^{-1} corresponds to CO_3^{2-} — H_2O stretching vibration, suggesting the presence of the water-molecule hydrogen bonded to the carbonate ions present in the interlayer of LDH. A band at about 1660 cm^{-1} can be ascribed to the bending vibration of H—O—H because of the presence

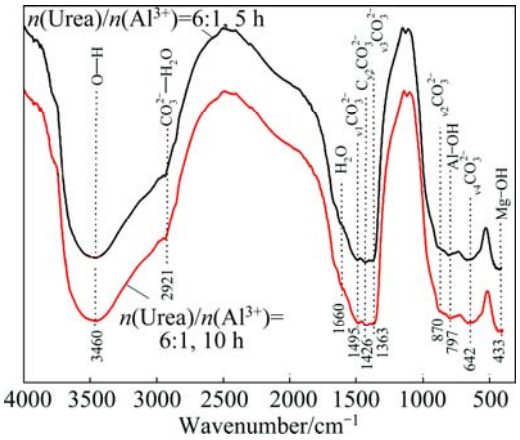

Fig. 5 FT-IR spectra of LDH films treated for 5 h and 10 h

of crystal water. The bands at 1495, 1426, 1363, 870 and 642 cm^{-1} are attributed to the symmetric and asymmetric stretching modes of CO_3^{2-} ion in the interlayer. Additionally, the bands at 797 cm^{-1} and 433 cm^{-1} can be due to the vibration modes of Al—OH and Mg—OH at the layer crystal lattice, respectively. These FT-IR results are in accordance with the results of XRD patterns.

The corrosion resistance of the films formed on AZ31 Mg alloy was investigated by potentiodynamic polarization curves measurements, and the lower the polarization current density, the better the corrosion resistance. Figure 6 shows the potentiodynamic polarization curves of the AZ31 Mg alloys treated at n(Urea)/n(Al^{3+})=6:1, for 5 h and 10 h and substrate in 3.5% NaCl aqueous solution. The free corrosion potentials (φ_{corr}) of the LDH-coated sample treated for 10 h and 5 h are −1.48 V and −1.41 V (vs SCE), respectively, much higher than that of the substrate, which is −1.55 V (vs SCE). And the corrosion current densities (J_{corr}) of the LDH-coated sample treated for 10 h and 5 h are 1.20×10^{-5} and 5.75×10^{-6} A/cm^2, respectively, which are lower than that of the AZ31 substrate (3.37×10^{-5} A/cm^2). It is obviously seen that the J_{corr} value of the LDH coated sample treated for 5 h decreased by one order of magnitude compared with the Mg alloy substrate. Also, there is a significant difference at the anodic branches of the curves. In the anodic branch of the polarization curve for the AZ31 substrate, a low breakdown potential (φ_b) is attributed to the breakdown of the oxidation film on the Mg surface. The J_{corr} raised rapidly with the increase in anodic potential higher than φ_b, indicating the active dissolution of the Mg substrate. However, the anodic branch of the coated sample treated for 5 h exhibits a passive trend. The J_{corr} increased slowly with increasing anodic potential. Thus, the potentiodynamic polarization results demonstrated that the LDH conversion film could effectively enhance the corrosion resistance of Mg alloys. In addition, when the

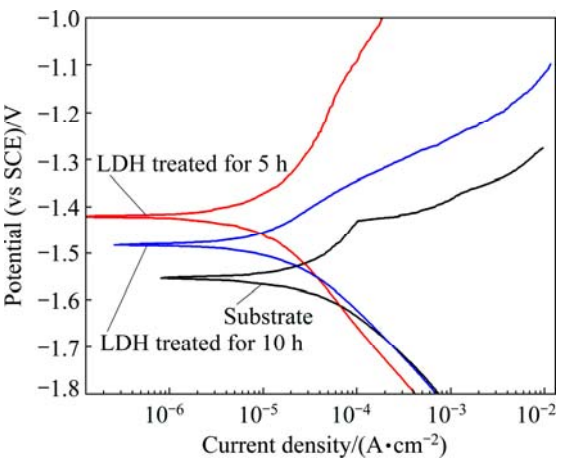

Fig. 6 Polarization curves of substrate, films treated for 5 h and 10 h

treatment time is prolonged, the J_{corr} decreased obviously. The cracks on the film formed by the hydrogen evolution increased with the immersion time, and seriously affected the compactness of the film.

The electrochemical impedance spectroscopy (EIS) was carried out to evaluate the corrosion resistance of the samples and investigate the structure of the films. Figures 7(a) and (b) show the Bode diagram and Nyquist plot, respectively. It is generally known that a higher Z modulus at the lower frequency and larger radius of the curvature represent better corrosion resistance on the metal substrates [38,39]. It can be seen from the Bode diagram that the samples treated for 5 h and 10 h show the bigger impedance at the low frequency than the substrate. Concurrently, it can be observed from the Nyquist plot (Fig. 7(b)) that the sample treated for 5 h shows the largest radius of the curvature and the sample treated for 10 h is also improved compared with the substrate. The LDH films with better EIS performance can effectively prevent the diffusion/penetration of the Cl^- ions to the Mg alloy substrate and thus reduce the corrosion rate of the substrate.

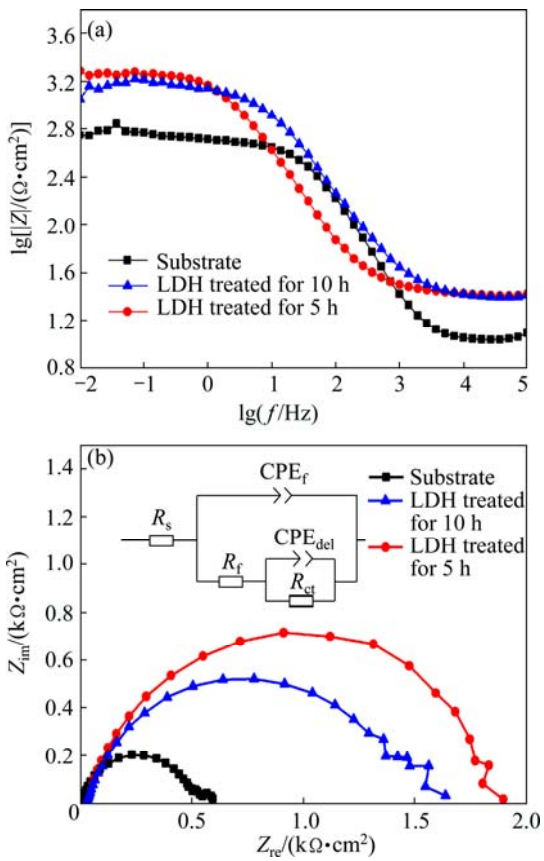

Fig. 7 Bode plots (a) and Nyquist plots with embedded equivalent electric circuit (b) of films and substrate

The EIS spectra were also analyzed based on the equivalent circuits as shown in Fig. 7(b). The data fitting results are listed in Table 2. R_s represents the solution

Table 2 Fitting results of EIS spectra for LDH films

Sample	R_s/ ($\Omega\cdot cm^2$)	R_f/ ($\Omega\cdot cm^2$)	Y_0/ ($\mu\Omega^{-1}\cdot cm^{-2}\cdot s^{-1}$)	n	R_{ct}/ ($\Omega\cdot cm^2$)	Y_0/ ($\mu\Omega^{-1}\cdot cm^{-2}\cdot s^{-1}$)	n'
Substrate	10.59	9.42	164.10	0.27	591	11.51	0.94
LDH treated for10 h	24.59	13.16	31.34	0.79	1456	360	1
LDH treated for 5 h	25.34	84.00	27.26	0.80	1839	4.22	0.83

resistance. Constant phase element (CPE) is used in place of a capacitor to compensate the non-homogeneity in the system, which is defined by Y_0 and n. If n is equal to 1, CPE is identical to a capacitor. R_f represents the resistance of the LDH film and CPE_f represents the capacitance of the LDH film. R_{ct} designates the charge transfer resistance and CPE_{del} designates the electric double layer capacity at the interface. Generally, the larger the value of R_{ct} is, the better the film performs. The value of R_{ct} for the substrate (591 $\Omega\cdot cm^2$) is much lower than those of the LDH coated samples treated for 10 h and 5 h, which are, 1456 and 1839 $\Omega\cdot cm^2$, respectively. It is indicated that the LDH film is very compact and effectively against the attack of Cl^- ions. The EIS data are perfectly accordance with the potentiodynamic polarization results, indicating that the LDH sample treated for 5 h has a higher corrosion resistance.

The XRD spectra of the LDH sample treated for 5 h before and after an immersion in 3.5% NaCl solution for 48 h are shown in Fig. 8(a). It is obvious that most of the peaks are the same between both samples, suggesting that the as-prepared LDH films possess excellent durability to corrosion. The XRD pattern of the immersed sample shows the $Mg(OH)_2$ peaks, implying the occurrence of corrosion between the LDH layer and the magnesium alloy substrate. Figure 8(b) shows the SEM morphology and its corresponding EDS spectrum of the immersed sample. The EDS spectrum of the exposed LDH film shows Cl and Na peaks in addition to Mg, Al, O and C elements after the immersion test. The result reveals that hydrotalcite presents the ion-exchange ability by absorbing Cl^- and Na^+ from NaCl solutions and the EDS results also display that the interlayer of hydrotalcite can retain Cl^- and Na^+ in the hydrotalcite structure. The SEM morphology (Fig. 8(b)) of the immersed LDH coated sample shows that the porous LDH film with vertical platelet-like microstructure was changed into a dense cladding.

As is well-known, chlorides, even in small amounts, typically damage the $Mg(OH)_2$ film on the Mg alloy surface continuously because of the replacement of OH^- ions with Cl^- ions and the high solubility of $MgCl_2$ in water [40,41]. The dissolution reaction of the $Mg(OH)_2$ film on the Mg alloy surface in chloride solution can be given as follows:

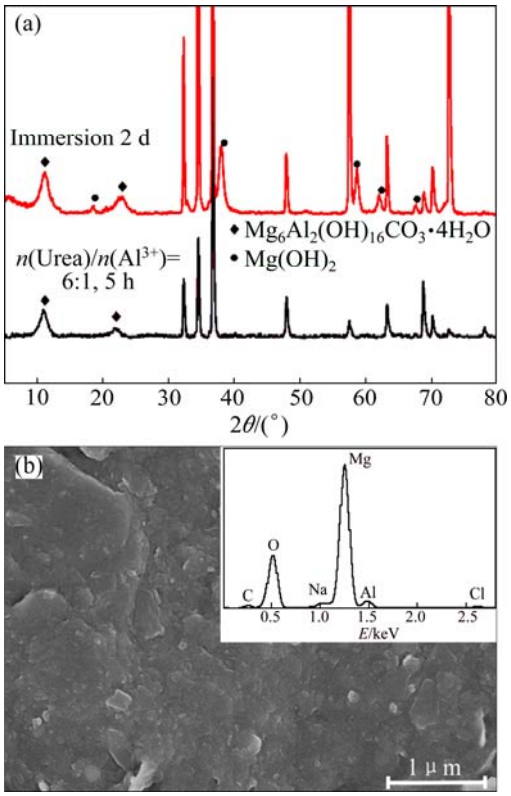

Fig. 8 XRD patterns (a), SEM morphology and its corresponding EDS spectrum (b) of immersed sample

$$Mg(OH)_2+Cl^-\rightarrow Mg(OH)Cl+OH^- \quad (1)$$

$$Mg(OH)Cl+Cl^-\rightarrow MgCl_2+OH^- \quad (2)$$

In contrast, with the common $Mg(OH)_2$ film, the developed LDH film had a much greater corrosion resistance because the existence of the ion-exchange capacity can protect the hydrotalcite structure from decomposition in the NaCl solution. The reason for the improvement in the corrosion performance of Mg alloys can be attributed to the absorption and retention of the aggressive Cl^- ions, and the release of the CO_3^{2-} ions. In conclusion, the ion-exchange reaction of the LDH film on the Mg alloy in chloride-containing solution can be expressed as follows:

$$LDH\text{-}CO_3^{2-}+2Cl^-\rightarrow LDH\text{-}2Cl^-+CO_3^{2-} \quad (3)$$

Figure 9 shows the XRD patterns of the LDH samples treated for 10 h with different ratios of urea to Al^{3+} ions. With an increase in the content of urea, in addition to these peaks of Mg and LDH phases, lots of

peaks attributed to the $Mg_5(CO_3)_4(OH)_2{\cdot}4H_2O$ and $MgCO_3$ structures are clearly observed. The existence of $Mg_5(CO_3)_4(OH)_2{\cdot}4H_2O$ and $MgCO_3$ structures is ascribed to the insufficient of the Al^{3+} ion in solution. Meanwhile, it reveals that $Mg_5(CO_3)_4(OH)_2{\cdot}4H_2O$ and $MgCO_3$ are the precursors during the formation of LDH film. A preliminary analysis of the growth process of the LDH film has been proposed on the basis of the XRD patterns. The possible reactions are listed as follows:

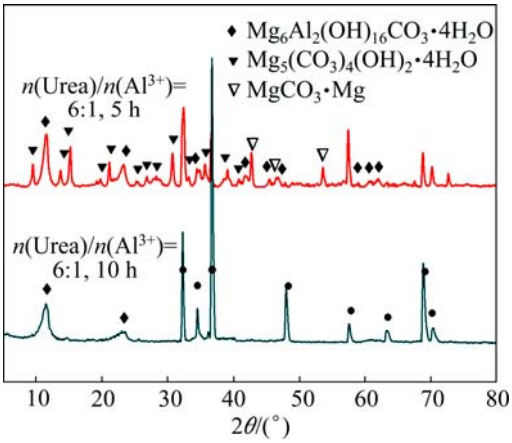

Fig. 9 XRD patterns of samples with different ratios of urea to Al^{3+} ions

Firstly, Al^{3+} ions hydrolyzed at a low temperature before urea decomposed:

$$Al^{3+}+3H_2O\rightarrow Al(OH)_3+3H^+ \quad (4)$$

At that condition, the pH value of the mixed solution was about 3.5. In such an acid solution, the dissolution of the magnesium led to the release of Mg^{2+} ions, accompanying with the hydrogen evolution.

Anodic reaction:

$$Mg\rightarrow Mg^{2+}+2e \quad (5)$$

Cathodic reaction:

$$2H_2O+2e\rightarrow 2OH^-+H_2\uparrow \quad (6)$$

At a temperature of 393 K, the urea underwent hydrolysis under high pressure and high temperature in the autoclave:

$$CO(NH_2)_2+4H_2O\rightarrow H_2CO_3+2NH_3{\cdot}H_2O \quad (7)$$

The pH value of the reaction system began to increase as the reaction progressed, and H_2CO_3 gradually translated into CO_3^{2-} ions, which reacted with the dissolved Mg^{2+} ions and thus led to the formation of $MgCO_3$. Subsequently, $MgCO_3$ deposited on the surface of the substrate:

$$H_2CO_3+2OH^-\rightarrow CO_3^{2-}+2H_2O \quad (8)$$

$$CO_3^{2-}+Mg^{2+}\rightarrow MgCO_3\downarrow \quad (9)$$

The urea continuously hydrolyzed such that CO_3^{2-} and OH^- ions developed into the system. Therefore, $MgCO_3$ translated into $Mg_5(CO_3)_4(OH)_2{\cdot}4H_2O$. It is known that $Mg_5(CO_3)_4(OH)_2{\cdot}4H_2O$ is a metastable hydrous carbonate and can be written as $4MgCO_3{\cdot}Mg(OH)_2{\cdot}4H_2O$. Also, CO_3^{2-} in $Mg_5(CO_3)_4(OH)_2{\cdot}4H_2O$ is more easily dissolved to form $Mg(OH)_2$ under the alkaline condition[42]:

$$Mg_5(CO_3)_4(OH)_2{\cdot}4H_2O+8OH^-\rightarrow 5Mg(OH)_2+4CO_3^{2-}+4H_2O \quad (10)$$

Finally, a part of Mg^{2+} ions in $Mg(OH)_2$ were replaced by Al^{3+} ions, and thus $Mg(OH)_2$ and $Al(OH)_3$ co-existed to form the more stable LDH structure [14,15]. Meanwhile, the OH^- ions in the interlayer were exchanged by CO_3^{2-} ions to form $Mg_6Al_2(OH)_{16}CO_3{\cdot}4H_2O$.

$$6Mg(OH)_2+2Al^{3+}+CO_3^{2-}+4OH^-+4H_2O\rightarrow Mg_6Al_2(OH)_{16}CO_3{\cdot}4H_2O \quad (11)$$

On the basis of experimental results, a model for the formation mechanism of the LDH film is illustrated in Fig. 10. Firstly, the dissolved Mg^{2+} ions deposited into the precursor film consisted of $MgCO_3$ and $Mg_5(CO_3)_4(OH)_2{\cdot}4H_2O$. Secondly, the precursor

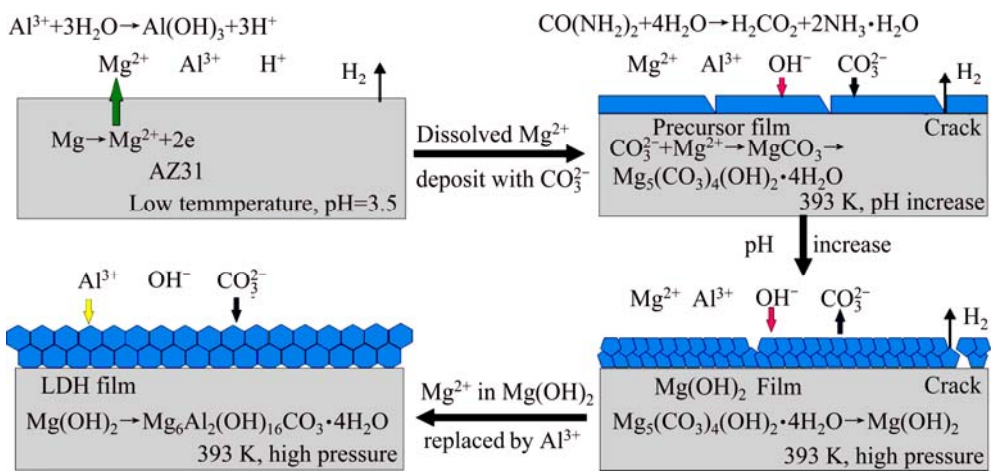

Fig. 10 Forming mechanism of film

translated into high crystalline $Mg(OH)_2$ in the alkaline conditions. Finally, the Mg^{2+} ions in $Mg(OH)_2$ was replaced by Al^{3+} ions, the $Mg(OH)_2$ translated into a more stable LDH structure, and meanwhile the OH^- in the interlayer was exchanged by CO_3^{2-}, thus led to the formation of the LDH ($Mg_6Al_2(OH)_{16}CO_3{\cdot}4H_2O$) film.

4 Conclusions

1) In-situ growth of nano-sized MgAl hydrotalcite conversion film on AZ31 alloy was developed by a one-step method with a urea hydrolysis process.

2) The LDH film, consisting of compact plate-like nanostructures and ion-exchange ability significantly improved the corrosion resistance of the AZ31 Mg alloy.

3) The formation mechanism of the LDH film was discussed. Firstly, the dissolved Mg^{2+} ions deposited into the precursor film consisted of $MgCO_3$ and $Mg_5(CO_3)_4(OH)_2{\cdot}4H_2O$; secondly, the precursor translated into the crystalline $Mg(OH)_2$ in alkaline conditions; finally, Mg^{2+} ions in $Mg(OH)_2$ were replaced by Al^{3+} ions, the $Mg(OH)_2$ translated into the more stable LDH structure, and meanwhile, the OH^- in the interlayer was exchanged by CO_3^{2-}, thus led to the formation of the LDH ($Mg_6Al_2(OH)_{16}CO_3{\cdot}4H_2O$) film.

References

[1] SONG Guang-ling, ATRENS A. Understanding magnesium corrosion — A framework for improved alloy performance [J]. Advanced Engineering Materials, 2003, 5: 837−858.

[2] ZENG Rong-chang, ZHANG Jin, HUANG Wei-jiu, DIETZEL W, KAINER K, BLAWERT C, KE Wei. Review of studies on corrosion of magnesium alloys [J]. Transactions of Nonferrous Metals Society of China, 2006, 16(4): 763−771.

[3] KIM W C, KIM J G, LEE J Y, SEOK H K. Influence of Ca on the corrosion properties of magnesium for biomaterials [J]. Materials Letters, 2008, 62: 4146−4148.

[4] SONG G. Recent progress in corrosion and protection of magnesium alloys [J]. Advanced Engineering Materials, 2005, 7: 563−586.

[5] MAKAR G L, KRUGER J. Corrosion studies of rapidly solidified magnesium alloys [J]. Journal of the Electrochemical Society, 1990, 137: 414−421.

[6] ZENG Rong-chang, SUN Xin-xin, SONG Ying-wei, ZHANG Fen, LI Shuo-qi, CUI hong-zhi, HAN En-hou. Influence of solution temperature on corrosion resistance of Zn−Ca phosphate conversion coating on biomedical Mg−Li−Ca alloys [J]. Transactions of Nonferrous Metals Society of China, 2013, 23(11): 3293−3299.

[7] GUO Hui-xia, MA Ying, WANG Jing-song, WANG Yu-shun, DONG Hai-rong, HAO Yuan. Corrosion behavior of micro-arc oxidation coating on AZ91D magnesium alloy in NaCl solutions with different concentrations [J]. Transactions of Nonferrous Metals Society of China, 2012, 22(7): 1786−1793.

[8] CHU Cheng-lin, HAN Xiao, BAI Jing, XUE Feng, CHU P K. Surface modification of biomedical magnesium alloy wires by micro-arc oxidation [J]. Transactions of Nonferrous Metals Society of China, 2014, 24(4): 1058−1064.

[9] ZHANG Xiao-xu, LI Qing, LI long-qin, ZHANG Peng, WANG Zhong-wei, CHEN Fu-nan. Fabrication of hydroxyapatite/stearic acid composite coating and corrosion behavior of coated magnesium alloy [J]. Materials Letters, 2012, 88: 76−78.

[10] XU Li-ping, YAMAMOTO A. Characteristics and cytocompatibility of biodegradable polymer film on magnesium by spin coating [J]. Colloids and Surfaces B: Biointerfaces, 2012, 93: 67−74.

[11] GRAY J, LUAN B. Protective coatings on magnesium and its alloys —A critical review [J]. Journal of alloys and compounds, 2002, 336: 88−113.

[12] SONG Ying-wei, SHAN Da-yong, CHEN Rong-shi, HAN En-hou. An environmentally friendly molybdate/phosphate black film on Mg−Zn−Y−Zr alloy [J]. Surface and Coatings Technology, 2010, 204: 3182−3187.

[13] YANG K H, GER M D, HWU W H, SUNG Y, LIU Y C. Study of vanadium-based chemical conversion coating on the corrosion resistance of magnesium alloy [J]. Materials Chemistry and Physics, 2007, 101: 480−485.

[14] CHEN Jun, SONG Ying-wei, SHAN Da-yong, HAN En-hou. Study of the in situ growth mechanism of Mg−Al hydrotalcite conversion film on AZ31 magnesium alloy [J]. Corrosion Science, 2012, 63: 148−158.

[15] CHEN Jun, SONG Ying-wei, SHAN Da-yong, HAN En-hou. In situ growth of Mg−Al hydrotalcite conversion film on AZ31 magnesium alloy [J]. Corrosion Science, 2011, 53: 3281−3288.

[16] CHEN Jun, SONG Ying-wei, SHAN Da-yong, HAN En-hou. Study of the corrosion mechanism of the in situ growth Mg−Al−CO_3^{2-} hydrotalcite film on AZ31 alloy [J]. Corrosion Science, 2012, 65: 268−277.

[17] CHEN Jun, SONG Ying-wei, SHAN Da-yong, HAN En-hou. Modifications of the hydrotalcite film on AZ31 Mg alloy by phytic acid: The effects on morphology, composition and corrosion resistance [J]. Corrosion Science, 2013, 74: 130−138.

[18] LIN Jun-kai, HSIA C L, UAN Jun-yen. Characterization of Mg, Al-hydrotalcite conversion film on Mg alloy and Cl^- and anion-exchangeability of the film in a corrosive environment [J]. Scripta Materialia, 2007, 56: 927−930.

[19] LIN Jun-kai, UAN Jun-yen. Formation of Mg, Al-hydrotalcite conversion coating on Mg alloy in aqueous HCO_3^-/CO_3^{2-} and corresponding protection against corrosion by the coating [J]. Corrosion science, 2009, 51: 1181−1188.

[20] LIN Jun-kai, JENG Kai-li, UAN Jun-yen. Crystallization of a chemical conversion layer that forms on AZ91D magnesium alloy in carbonic acid [J]. Corrosion Science, 2011, 53: 3832−3839.

[21] LIN Jun-kai, UAN Jun-yen, WU Chia-ping, HUANG Her-hsiung. Direct growth of oriented Mg–Fe layered double hydroxide (LDH) on pure Mg substrates and in vitro corrosion and cell adhesion testing of LDH-coated Mg samples [J]. Journal of Materials Chemistry, 2011, 21: 5011−5020.

[22] SYU Jia-han, UAN Jun-yen, LIN Meng-chang, LIN Zhi-yu. Optically transparent Li−Al−CO_3^{2-} layered double hydroxide thin films on an AZ31 Mg alloy formed by electrochemical deposition and their corrosion resistance in a dilute chloride environment [J]. Corrosion Science, 2012, 68: 238−248.

[23] UAN Jun-yen, LIN Jun-kai, SUN Ying-sui, YANG Wei-en, CHEN Li-kai, HUANG Her-hsiung. Surface coatings for improving the corrosion resistance and cell adhesion of AZ91D magnesium alloy through environmentally clean methods [J]. Thin Solid Films, 2010, 518: 7563−7567.

[24] UAN Jun-yen, YU Bing-lung, PAN Xin-liang. Morphological and microstructural characterization of the aragonitic $CaCO_3$/Mg, Al-hydrotalcite coating on Mg-9 Wt Pct Al-1 Wt Pct Zn alloy to protect against corrosion [J]. Metallurgical and Materials Transactions A, 2008, 39: 3233−3245.

[25] ZHANG Fen, LIU Zhen-guo, ZENG Rong-chang, LI Shuo-qi, CUI Hong-zhi, SONG Liang, HAN En-hou. Corrosion resistance of

Mg−Al-LDH coating on magnesium alloy AZ31 [J]. Surface and Coatings Technology, 2014, 258: 1152−1158.

[26] ZENG Rong-chang, LIU Zhen-guo, ZHANG Fen, LI Shuo-qi, CUI Hong-zhi, HAN En-hou. Corrosion of molybdate intercalated hydrotalcite coating on AZ31 Mg alloy [J]. Journal of Materials Chemistry A, 2014, 2: 13049−13057.

[27] HSIEH Zhi-lun, LIN Meng-chang, UAN Jun-yen. Rapid direct growth of Li–Al layered double hydroxide (LDH) film on glass, silicon wafer and carbon cloth and characterization of LDH film on substrates [J]. Journal of Materials Chemistry, 2011, 21: 1880−1889.

[28] CHEN Hong-yun, ZHANG Fa-zhi, CHEN Tao, XU Sai-long, EVANS D G, DUAN Xue. Comparison of the evolution and growth processes of films of M/Al-layered double hydroxides with M= Ni or Zn [J]. Chemical Engineering Science, 2009, 64: 2617−2622.

[29] LIU Jin-ping, LI Yuan-yuan, HUANG Xin-tang, LI Guang-yun, LI Zi-kun. Layered double hydroxide nano- and microstructures grown directly on metal substrates and their calcined products for application as Li^+ ion battery electrodes [J]. Advanced Functional Materials, 2008, 18 : 1448−1458.

[30] YU Bing-lung, LIN Jun-kai, UAN Jun-yen. Applications of carbonic acid solution for developing conversion coatings on Mg alloy [J]. Transactions of Nonferrous Metals Society of China, 2010, 20(7): 1331−1339.

[31] HIBINO T, OHYA H. Synthesis of crystalline layered double hydroxides: Precipitation by using urea hydrolysis and subsequent hydrothermal reactions in aqueous solutions [J]. Applied Clay Science, 2009, 45: 123−132.

[32] OGAWA M, KAIHO H. Homogeneous precipitation of uniform hydrotalcite particles [J]. Langmuir, 2002, 18: 4240−4242.

[33] OH J M, HWANG S H, CHOY J H. The effect of synthetic conditions on tailoring the size of hydrotalcite particles [J]. Solid State Ionics, 2002, 151: 285−291.

[34] OKAMOTO K, IYI N, SASAKI T. Factors affecting the crystal size of the MgAl-LDH (layered double hydroxide) prepared by using ammonia-releasing reagents [J]. Applied Clay Science, 2007, 37: 23−31.

[35] LI Shi-feng, SHEN Yan-ming, LIU Dong-bin, FAN Li-hui, ZHENG Xin-cai, YANG Ju-an. One-step fabrication of oriented Mg/Al-layered double hydroxide film on magnesium substrate with urea hydrolysis and its corrosion resistance [J]. Composite Interfaces, 2012, 19: 489−498.

[36] WANG Li-da, ZHANG Kai-yue, SUN Wen, WU Ting-ting, HE Hao-ran, LIU Gui-chang. Hydrothermal synthesis of corrosion resistant hydrotalcite conversion coating on AZ91D alloy [J]. Materials Letters, 2013, 106: 111−114.

[37] ISHIZAKI T, CHIBA S, WATANABE K, SUZUKI H. Corrosion resistance of Mg–Al layered double hydroxide container-containing magnesium hydroxide films formed directly on magnesium alloy by chemical-free steam coating [J]. Journal of Materials Chemistry A, 2013, 1: 8968−8977.

[38] VREUGDENHIL A, GELLING V, WOODS M, SCHMELZ J, ENDERSON B. The role of crosslinkers in epoxy–amine crosslinked silicon sol−gel barrier protection coatings [J]. Thin Solid Films, 2008, 517: 538−543.

[39] QIAN Min, MCINTOSH S A, TAN Xiu-hui, ZENG Xian-ting, WIJESINGHE S L. Two-part epoxy-siloxane hybrid corrosion protection coatings for carbon steel [J]. Thin Solid Films, 2009, 517: 5237−5242.

[40] GHALI E, DIETZEL W, KAINER K. General and localized corrosion of magnesium alloys: A critical review [J]. Journal of Materials Engineering and Performance, 2004, 13: 7−23.

[41] AVEDESIAN M M, BAKER H. ASM specialty handbook: Magnesium and magnesium alloys [M]. Ohio: ASM International, 1999: 199.

[42] ZENG Rong-chang, HU Yan, GUAN Shao-kang, CUI Hong-zhi, HAN En-hou. Corrosion of magnesium alloy AZ31: The influence of bicarbonate, sulphate, hydrogen phosphate and dihydrogen phosphate ions in saline solution [J]. Corrosion Science, 2014, 86: 171−182.

AZ31 镁合金表面一步法合成原位镁铝水滑石转化膜

曾荣昌[1,2]，刘振国[1,2]，张 芬[1,2]，李硕琦[1,2]，赫庆坤[1]，崔洪芝[1]，韩恩厚[3]

1. 山东科技大学 材料科学与工程学院，青岛 266590；
2. 山东科技大学 省部共建矿山灾害预防控制国家重点实验室，青岛 266590；
3. 中国科学院 金属研究所，沈阳 110016

摘 要：通过尿素水解法在 AZ31 镁合金表面原位合成纳米尺度的层状双金属氢氧化物(水滑石)转化膜，并提出成膜机理。首先，溶解的 Mg^{2+}离子沉积形成含有 $MgCO_3$ 和 $Mg_5(CO_3)_4(OH)_2·4H_2O$ 的前驱体膜；然后，前驱体膜在碱性条件下转化为高结晶的 $Mg(OH)_2$；最后，$Mg(OH)_2$ 中的 Mg^{2+}离子被 Al^{3+}离子取代，$Mg(OH)_2$ 转化为更稳定的水滑石层状结构，同时层间 OH^-与溶液中的 CO_3^{2-} 发生离子交换，因此形成水滑石($Mg_6Al_2(OH)_{16}CO_3·4H_2O$)膜。结果表明，以互锁的片状纳米结构和离子交换性能为特征的水滑石膜可以有效提高 AZ31 镁合金的耐蚀性。

关键词：镁合金；水滑石；转化膜；耐蚀性；离子交换

(Edited by Xiang-qun LI)